Journal of Solid State Chemistry **147,** 520–526 (1999)
Article ID jssc.1999.8411, available online at http://www.idealibrary.com on IDEAL®

Reactivity of a New Zirconium Phosphonate Phase, $Zr_2(O_3P\text{-}CH_2CH_2\text{-bipyridinium-}CH_2CH_2\text{-}PO_3)X_6 \cdot 2H_2O$, Toward Organic and Inorganic Monophosphonates

Lori A. Vermeulen[1] and Scott J. Burgmeyer

Department of Chemistry and Biochemistry, Southern Illinois University, Carbondale, Illinois 62901-4409

Received February 1, 1999; in revised form May 24, 1999; accepted May 27, 1999

We report that zirconium viologen diphosphonate, ($Zr_2(O_3P\text{-}CH_2CH_2\text{-bipyridinium-}CH_2CH_2\text{-}PO_3)X_6 \cdot 2H_2O$), where X = halide ion, ZrVP, will react with a variety of phosphonates ($H_2O_3P\text{-}R$, where R = OH, H, CH_3, C_6H_5) under mild conditions, producing a disordered porous phase. This is in sharp contrast to the observed reactivity of the more common zirconium phosphonate phases: the α-phase group (IVB) layered phosphonates $Zr(O_3PR)_2$ (whose structures are based upon α-($Zr(O_3POH)_2 \cdot H_2O$), α-ZrP) are resistant to reaction with monophosphonates while γ-$Zr(O_4P)(O_2P(OH)_2) \cdot 2H_2O$, γ-ZrP, undergoes topotactic ligand exchange with mono- and di-phosphonates to form ordered porous materials. We follow the reaction by X-ray powder diffraction and IR and UV spectroscopies and investigate the porous nature of the resulting solids through ion-exchange and N_2 adsorption experiments. © 1999 Academic Press

INTRODUCTION

Layered metal phosphonates ($M(O_3P\text{-}R)_2 \cdot mH_2O$ or $M(O_3P\text{-R-}PO_3) \cdot mH_2O$ where M = tetravalent metal and R = organic group, H, or OH) have great potential as construction tools in the design of new materials that can be utilized for many different applications, ranging from heterogeneous catalysis to optoelectronics (1–4). The structure of the layered metal phosphonates typically resembles that of their inorganic analog α-$Zr(O_3POH)_2 \cdot H_2O$, α-**ZrP**, where the inorganic layer is constructed by linking phosphonate tetrahedra. In the analogous $M(O_3P\text{-}R)_2 \cdot mH_2O$ solids, adjacent inorganic layers are held together by van der Waals interactions. Alternatively, covalent bonds link adjacent inorganic layers in the metal diphosphonates, $M(O_3P\text{-}R\text{-}PO_3) \cdot mH_2O$. Metal phosphonates have good thermal stability and can be prepared in bulk as microcrystalline solids. In addition, thin films of the general formula $M(O_3P\text{-}R\text{-}PO_3)$ can be constructed from the metal and diphosphonate building blocks one molecular layer at a time (5).

The group (IVB) metal phosphonates are very versatile in the sense that a variety of R groups can be incorporated, thereby allowing for the design of interesting inorganic/organic composite materials with tailored properties. In general, the metal phosphonates will adapt the α-**ZrP** structure so long as the appended R group can fit in the 25 Å^2 space allowed by the host lattice (1). However, it has recently been observed that other crystalline phases may form when R is too bulky (6) or if R is charged (7). This is true for the title compound zirconium viologen diphosphonate, $Zr_2(O_3P\text{-}CH_2CH_2\text{-bipyridinium-}CH_2CH_2\text{-}PO_3)X_6 \cdot 2H_2O$, where X = halide, **ZrVP**, in which the zirconium phosphonate obtained is constructed from the doubly-charged bis(N,N′-diethylviologenphosphonic acid), **VP**, whose molecular conformation is shown in Fig. 1 (7). The resulting solid contains a 1:1 ratio of Zr:P, in contrast to the 1:2 ratio observed in the typical α-phase. The structure is layered but the layers consist of double chains of $Zr(X_3O_3)$ octahedra where the oxygen atoms originate from the phosphonate groups of three different **VP** molecules as shown schematically in Fig. 2. It is believed that this new structure is directed by charge–charge repulsions which are minimized compared to the unfavorable interactions that would result due to the close proximity of the viologen moieties if the α-phase were to form.

In this paper we report our investigation of the reactivity of **ZrVP** toward a series of phosphonic acids ($H_2O_3P\text{-}R$, where R = OH, H, CH_3, C_6H_5). It has been reported that compounds of the α-**ZrP** structure are resistant to reaction with phosphonates unless forcing conditions are utilized (8). On the other hand, it has been shown that for γ-($Zr(O_4P)(O_2P(OH)_2) \cdot 2H_2O$), γ-**ZrP**, ligand exchange of the dihydrogen phosphate group occurs in a topotactic fashion resulting in the formation of well-ordered porous materials (9–17). In contrast, here we show that **ZrVP** undergoes

[1]To whom correspondence should be addressed. Fax: 618-453-6408. E-mail: vermeulen@chem.siu.edu.

0022-4596/99 $30.00

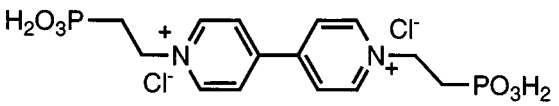

FIG. 1. Structure of **VP**, bis(N,N′-diethyviologenphosphonic acid).

reactions with phosphonates under mild conditions, producing disordered phases that are porous. The evidence suggests that this transformation occurs through a dissolution–reprecipitation reaction rather than by topotactic exchange. The reactions are followed by X-ray diffraction, IR, and UV spectroscopies. The porous nature of the resulting solids is investigated by ion exchange experiments and N_2 adsorption measurements.

EXPERIMENTAL

All chemicals were used as received.

Synthesis of viologen diphosphonate ($H_2O_3PCH_2CH_2$-4,4′ *bipyridinium*-$CH_2CH_2PO_3H_2Cl_2^-$), **VP**. Viologen diphosphonate was prepared as reported previously (18) from diethylbromoethylphosphonate (25 g) (Acros) and 4,4′ bipyridine (7.35 g) (Aldrich), followed by hydrolysis with HCl (^{1}H NMR, D_2O, ppm: 2.2 *m*, 4.0 *m*, 8.6 *d*, 9.2 *d*).

Synthesis of zirconium viologen phosphonate ($Zr_2(O_3P$-CH_2CH_2-*bipyridinium*-CH_2CH_2-$PO_3)X_6 \cdot 2H_2O$), ***ZrVP***. Zirconium viologen phosphonate was prepared as reported previously (7) from $ZrOCl_2 \cdot 8H_2O$ (0.92 g) (Aldrich), 50% HF (0.484 g) (Baker) and viologen diphosphonate (X-ray, 2θ, degrees: 9.6, 14.0, 15.0, 15.5, 17.8, 19.7, 21.2, 22.9, 24.6, 25.0, 26.8, 27.3, 27.6, 35.0, Fig. 3A) (IR, KBr, cm^{-1}: 3130, 3048, 1637, 1554, 1501, 1443, 1390, 1161, 1055, 826, 767, 544, 503, Fig. 7).

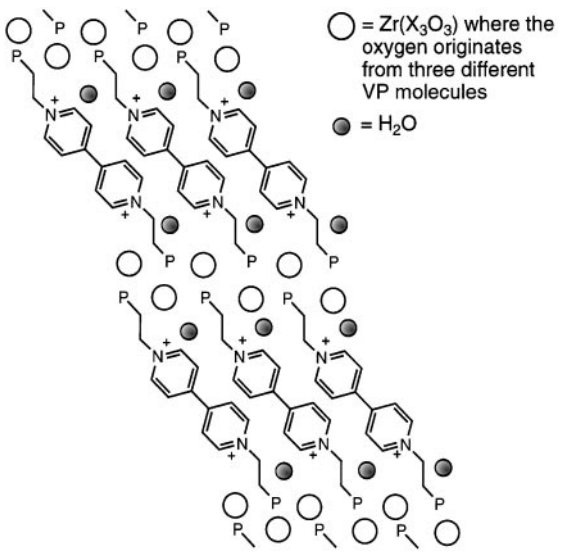

FIG. 2. Schematic representation of the structure of **ZrVP**, ($Zr_2(O_3P$-CH_2CH_2-bipyridinium-CH_2CH_2-$PO_3)X_6 \cdot 2H_2O$), where X = halide ion.

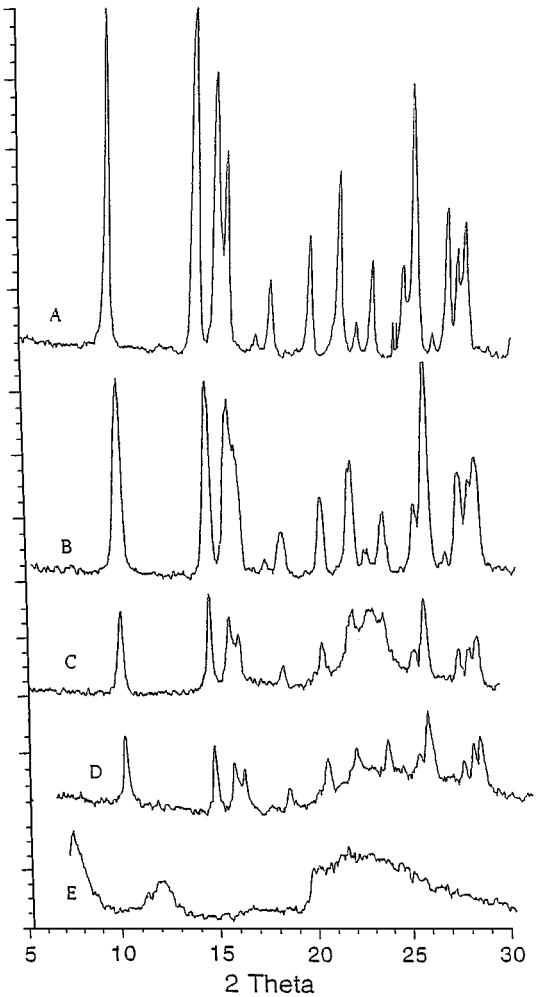

FIG. 3. X-ray powder diffraction patterns of **ZrVP** after treatment with 1 M H_2O_3POH at 25°C for (A) zero h, (B) 12 h, (C) 24 h, (D) 48 h, and (E) 96 h.

Displacement reactions. **ZrVP** (0.5 g) was stirred in a 1 M solution (50 mLs) of H_2O_3PR where R = OH, H, CH_3, and C_6H_5 at room temperature. Samples were removed by filtration at various times for analysis by X-ray and IR. The reaction was also carried out in 1 M phosphoric acid at reflux for seven days.

Kinetic studies. **ZrVP** (0.200 g) and 50 mL of 1 M H_3PO_4 were placed in a centrifuge tube and stirred at room temperature. Every 30–60 min the stirring was stopped and the centrifuge tube was spun at 7000 rpm for 3 min. Exactly 0.50 mL of the supernatant was pipetted out and diluted to 50 mL. A UV/vis spectra was obtained and the absorbance determined. Concentration of **VP** in solution was determined from a standard curve.

Ion exchange. Samples of **ZrVP** and the solid product of the displacement reactions were treated with a solution of potassium iodide at room temperature. The solids were removed by filtration, washed with water, and the color was observed.

Instrumentation. X-ray powder diffraction patterns were obtained with a Norelco high-angle powder diffractometer using Ni-filtered Cu$K\alpha$ radiation at a scan rate of 1° per minute. The samples were packed into a standard aluminum holder. IR spectra (KBr) were obtained on a Perkin–Elmer 1600 series FTIR. UV/vis spectra were executed on a Shimatzu UV/vis Spectrometer. Samples for SEM were sputtered with a gold-palladium alloy prior to imaging with a Hitachi S2460N variable-pressure scanning electron microscope in high-vacuum mode at a magnification of 200×. Surface area measurements were performed using a NOVA-1200 BET Surface Area Analyzer with nitrogen as the sorbent. After outgassing, the BET surface analysis was carried out at the temperature of 77 K. The multipoint BET surface area, average pore diameter, and pore size distribution were calculated using the Quantachrome software.

RESULTS AND DISCUSSION

The X-ray powder diffraction pattern of **ZrVP** is shown in Fig. 3A and matches that previously reported for this material (7). Upon treatment of **ZrVP** with 1 M phosphoric acid at reflux for seven days, the powder pattern is completely changed (Fig. 4). A more gradual change in the X-ray powder pattern is observed when this reaction is carried out at room temperature. The gradual broadening of the diffraction peaks is shown in Figs. 3B–3E for samples treated with phosphoric acid for 12, 24, 48, and 96 h. The pattern that is

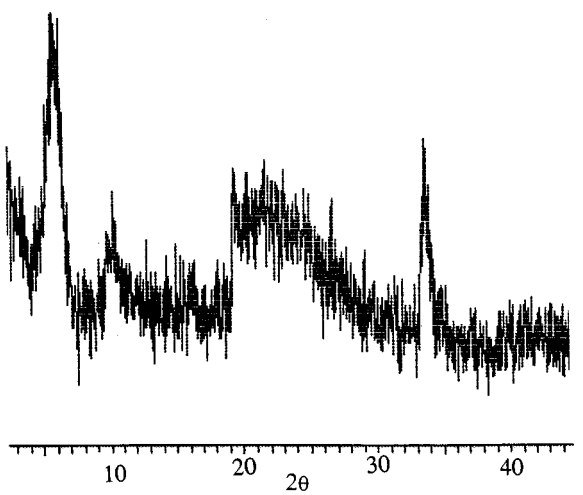

FIG. 4. X-ray powder diffraction pattern of **ZrVP** after treatment with 1 M H_2O_3POH for 7 days at reflux.

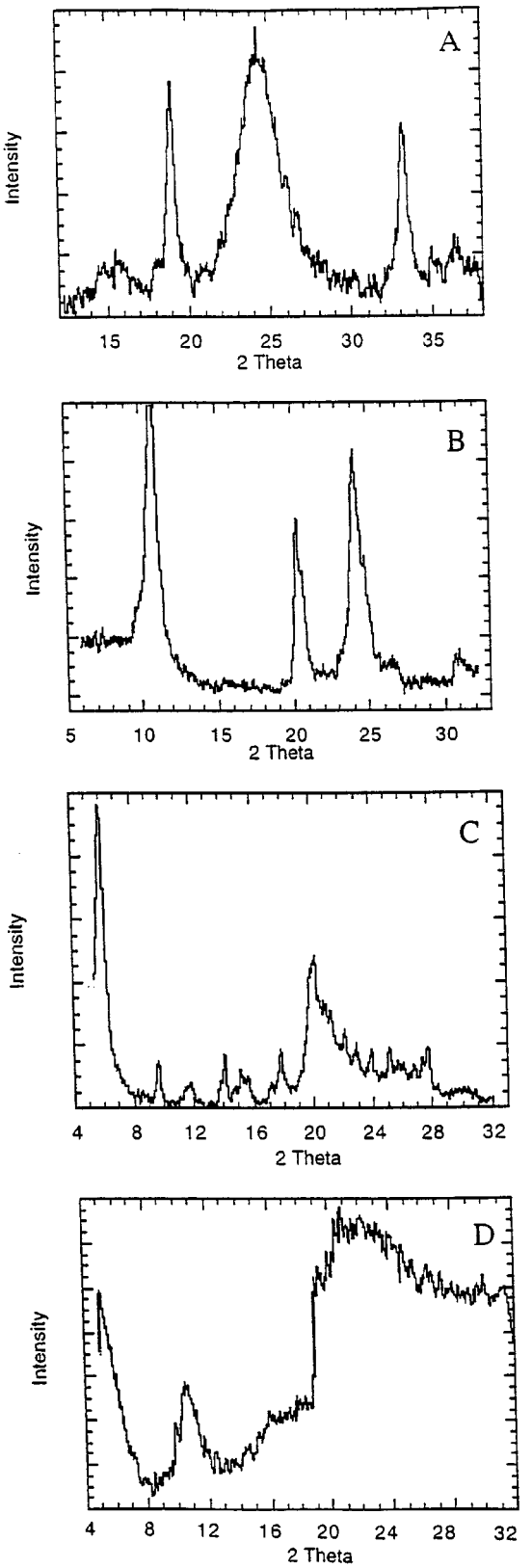

FIG. 5. X-ray powder diffraction patterns of **ZrVP** after treatment with 1 M H_2O_3PR at 25°C for 120 h: (A) R = H, (B) $R = CH_3$, (C) $R = C_6H_5$, and (D) R = OH.

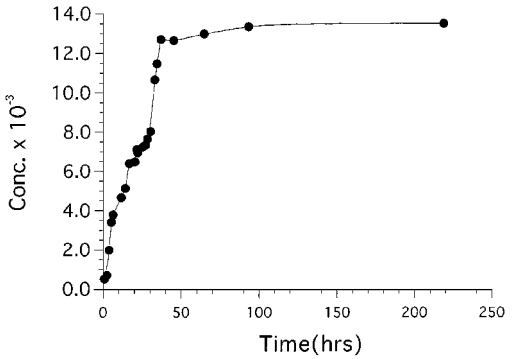

FIG. 6. Kinetic profile for the reaction of **ZrVP** with 1 M H_2O_3POH at 25°C. (The concentration of **VP** is determined by UV/vis spectroscopy.)

observed for the sample of **ZrVP** treated for 5 days at room temperature (Fig. 3E) is qualitatively similar to that observed for the sample treated for 7 days at reflux (Fig. 4).

The reaction was investigated using a variety of phosphonates (H_2O_3PR, where $R = OH$, H, CH_3, C_6H_5) at room temperature. As can be seen in Fig. 5, the X-ray powder pattern of each is considerably changed after 5 days of reaction in 1 M solution of the phosphonic acid at room temperature. After reaction with phosphoric, phosphorous, and methyl phosphonic acids, there is no evidence for crystalline **ZrVP** remaining after 5 days. There are some diffraction peaks due to **ZrVP** still observable for the sample

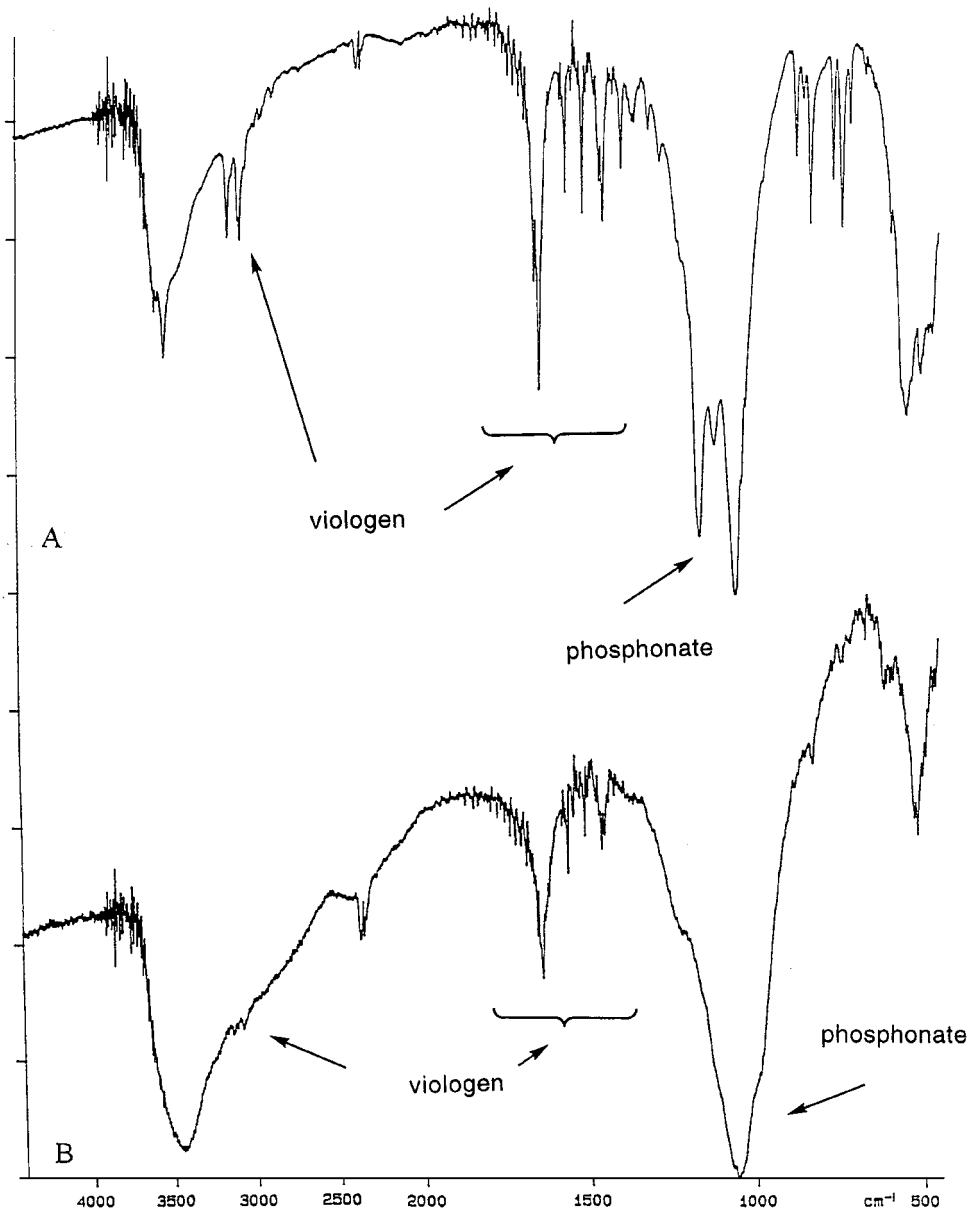

FIG. 7. IR Spectra of (A) **ZrVP** and (B) solids recovered after treatment of **ZrVP** with 1 M H_2O_3POH at 25°C for 120 h.

treated with phenyl phosphonic acid, although these peaks are significantly broadened.

After treatment of **ZrVP** with all of the phosphonates studied, a peak appears in the X-ray powder pattern at low 2θ that is close to that which would be expected for the reaction of the phosphonate (H_2O_3PR) and zirconium (Fig. 5). For example, in the powder pattern obtained from **ZrVP** treated with phosphorous acid (Fig. 5A), the broad peaks located at $2\theta = 18.9°$, 24.2°, and 33.1° are similar to diffraction peaks reported for crystalline $Zr(O_3PH)_2$, although they are significantly broadened (19). In a similar fashion, evidence for $Zr(O_3P\text{-}R)_2$ is found in each powder pattern ($Zr(O_3P\text{-}CH_3)$, $d = 10.7$ Å (20); $Zr(O_3PC_6H_5)_2$, $d = 15.0$ Å (19); $Zr(O_3POH)_2$, $d = 9$ Å (19)). In each case, the peaks are broader than those reported for crystalline $Zr(O_3PR)_2$ prepared in refluxing aqueous HF and provide a slightly higher interlayer distance, indicating that these phases are not well ordered and are probably hydrated.

We were able to show by UV spectroscopy that the viologen diphosphonate, **VP**, was removed from the solid over the course of the reaction. A plot of concentration of **VP** in the supernatant versus time is shown in Fig. 6 for the reaction of **ZrVP** with phosphoric acid at room temperature. The **VP** concentration in the supernatant increases abruptly at first over the first several hours (rate = approximately 1×10^{-3} M/min) and then continues to increase at a slower rate for the first 40 h. The concentration of the supernatant remains constant after approximately 40 h. If we calculate the total amount of **VP** that is present in the supernatant after the concentration has reached a constant value, we see that it is equal to 52% of that present in the original **ZrVP** solid.

The IR spectrum of **ZrVP** is shown in Fig. 7. After treatment with 1 M phosphoric acid at room temperature, significant changes in the IR spectrum of the solid are observed. Notably, the peaks which correspond to the organic groups (aromatic viologen stretches and aliphatic stretches and bends) are decreased in intensity relative to the peaks attributed to the phosphonate functionality. A gradual change in peak intensity is observed over time. After the reaction is over (as determined by the kinetic study), there are still peaks observed that are representative of the organic group, corroborating the calculation described above.

A qualitative test was performed in which the phosphonate-treated solids were treated with a solution of basic sodium dithionite. The characteristic blue color of reduced viologen was observed in every case. This test confirms that **VP** remains in the solid after **ZrVP** is treated with another phosphonate for 5 days at room temperature.

The X-ray, IR, and UV experiments indicate that **ZrVP** is easily converted to other solid state materials when it is treated with a variety of phosphonic acids under very mild conditions. The X-ray evidence supports the formation of a disordered $Zr(O_3PR)_2$ phase. The disappearance of crystalline **ZrVP** and detection of **VP** in the supernatant indicates that the solid at least partially dissolves under these conditions, liberating **VP** and zirconium ions. The disordered $Zr(O_3PR)_2$ phase likely results from the reaction of the liberated zirconium ions and the phosphonate that is in excess (H_2O_3PR). This dissolution–reprecipitation mechanism is further supported by a marked decrease in particle size of the solids as observed by SEM. Images that were obtained both before and after the reaction with phosphoric acid are shown in Fig. 8. When a control experiment is performed by stirring **ZrVP** in water at room temperature for 5 days, there is no comparable broadening in the X-ray powder pattern or decrease in particle size.

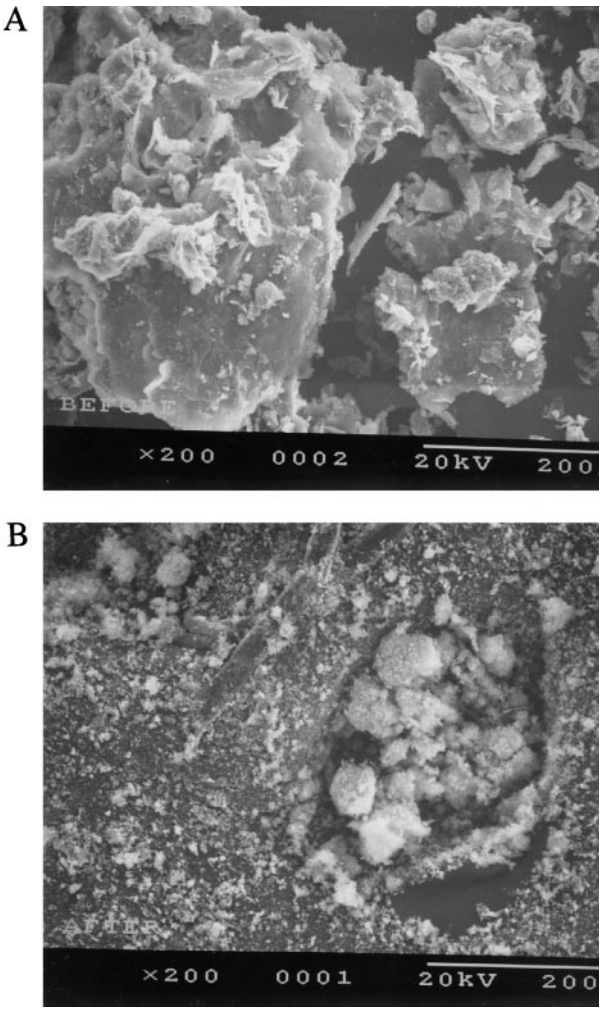

FIG. 8. SEM images of (A) **ZrVP** and (B) solids recovered after treatment of **ZrVP** with 1 M H_2O_3POH at 25°C for 120 h.

The evidence (IR, UV, and chemical reduction) shows that **VP** remains in the solid products after there are no longer changes in the X-ray powder patterns and concentration of **VP** in the supernatant. However, there is no evidence

in the X-ray powder pattern for crystalline **ZrVP**. In order to gain some insight into the nature of the solid remaining that contains **VP**, we performed a simple ion exchange experiment. It is well known that viologens form charge-transfer salts with halides, giving rise to an intense absorption band which shifts to lower energies as the halide is changed through the series, Cl^-, Br^-, I^- (21). Thus, when **VP** is mixed with a solution of potassium iodide, a yellow color becomes immediately visible. However, when solid **ZrVP** is treated with a saturated solution of potassium iodide, there is *no* visible color change. This is easily understood when one considers the structure of the **ZrVP** solid (7). Because the counteranions for the viologen cationic centers are complex ions that are actually part of the lattice, $[Zr(O_3P\text{-}R)(X_3)]^{1-}$ (where *R* refers to the viologen moiety and *X* refers to halide), ion exchange is impossible. However, when the solid product of the displacement reaction of **ZrVP** and phosphoric acid is stirred in a solution of potassium iodide, a bright yellow solid results. This observation is consistent with the formation of a disordered, potentially porous solid, in which the viologen moiety and counterion are accessible to ion-exchange.

To determine whether or not these materials are indeed porous, N_2 adsorption measurements were carried out for samples that had been treated with all four of the phosphonic acids studied. The results are shown in Table 1. All of the surface areas had increased compared to **ZrVP** (except for the reaction with phenyl phosphonic acid). The increase in surface area and in total pore volume depends upon the side group R of the added monophosphonate according to the trend $-H > -CH_3 > -OH > -C_6H_5$. This trend suggests the possibility that the reaction depends to some extent upon diffusion of the monophosphonate into the **ZrVP** solid and thus the size of the appended *R* group. The average pore radius and pore distribution are small and narrow for the products of the reaction with the phosphor-

TABLE 1
BET Porosity Measurements of Solids obtained from Reaction of ZrVP with H_2O_3P-*R*

–*R*	Surface area increase (compared to **ZrVP**)	Total pore volume	Average pore radius
–H	42.1 m^2/g	137×10^{-3} mL/g	1.9 Å
$-CH_3$	25.9m^2/g	73.7×10^{-3} mL/g	5.0 Å
–OH	2.19 m^2/g	49.9×10^{-3} mL/g	456 Å
$-C_6H_5$	0 m^2/g	—	—

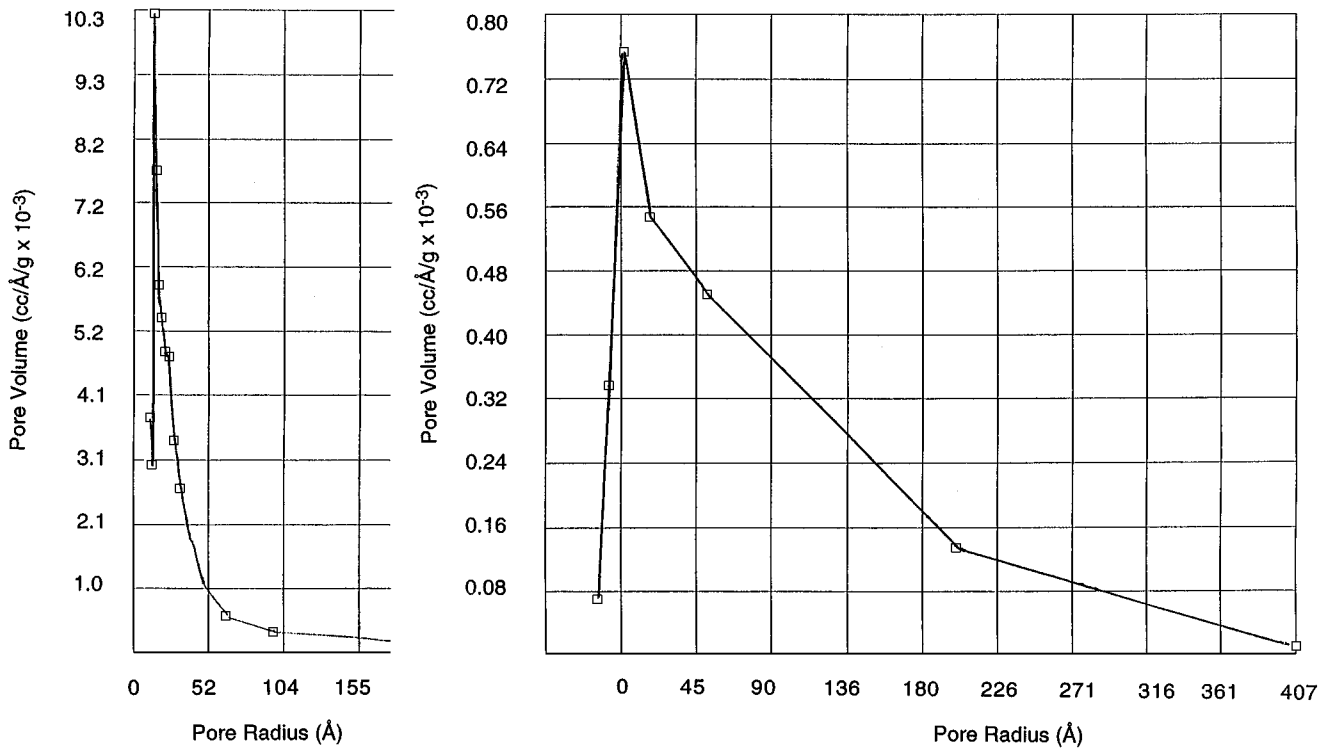

FIG. 9. Differential pore volume as a function of the pore radius (left) after treatment of **ZrVP** with 1 M H_2O_3PH and (right) after treatment of **ZrVP** with 1 M H_2O_3POH.

ous and methyl phosphonic acids compared to the large average pore diameter and broad pore size distribution for the product of the reaction with phosphoric acid (Fig. 9).

The interpretation of the N_2 adsorption experiments is complicated by the fact that there are a mixture of products obtained, a disordered $Zr(O_3PR)_2$ phase, and a disordered material that contains the viologen phosphonate. The presence of porosity in the viologen phase is consistent with the ion-exchange behavior; however, some of the measured porosity may be due to the formation of the disordered $Zr(O_3PR)_2$ phase. In related work, we have observed that thin films constructed from alternate depositions of **VP** and zirconium ions on quartz substrates also are reactive upon treatment with a series of phosphonic acids, liberating **VP** in solution. The rate of reaction is also related to the size of the appended *R* group on the monophosphonate (23). Our current work involves the study of the porous nature of these films by quartz crystal gravimetry. The films treated with monophosphonates should not be contaminated with a $Zr(O_3PR)_2$ phase, and thus adsorption experiments will be easier to interpret.

CONCLUSIONS

We have shown that **ZrVP** reacts with a variety of phosphonic acids under very mild conditions, resulting in the production of a disordered $Zr(O_3PR)_2$ phase and a disordered zirconium phosphonate phase that contains **VP**. This observation is in sharp contrast to the reactivity of the other common zirconium phosphonate phases which are either resistant to reaction or react in a topotactic fashion to produce ordered porous phases. The viologen materials are potentially useful as catalysts and photovoltaics (24–28), and further study of their reactivity as both solids and thin films is warranted.

ACKNOWLEDGMENTS

The authors gratefully acknowledge the Materials Technology Center at SIUC and the Petroleum Research Fund administered by the American Chemical Society for support of this work. We acknowledge Paul Robinson for help with obtaining the X-ray powder diffraction data, Tomek Wiltowski from the Coal Research Center for assistance with the N_2 BET measurements, and the Electron Microscopy Center at SIUC for the SEM images.

REFERENCES

1. A. Clearfield, *in* "Progress in Inorganic Chemistry" (K. D. Karlin, Ed.), Vol. 47, p. 371. Wiley, New York, 1998.
2. G. Alberti, M. Casciola, U. Costantino, and R. Vivani, *Adv. Mater.* **8,** 291 (1996).
3. M. E. Thompson, *Chem. Mater.* **6,** 1168 (1994).
4. G. Cao, H. Hong, and T. E. Mallouk, *Acc. Chem. Res.* **25,** 420 (1992).
5. H. Lee, J. Kepley, H.-G. Hong, and T. E. Mallouk, *J. Am. Chem. Soc.* **110,** 1567 (1988).
6. B. Zhang, D. M. Poojary, A. Clearfield, and G. Z. Peng, *Chem. Mater.* **8,** 1333 (1996).
7. D. M. Poojary, L. A. Vermeulen, E. Vicenzi, A. Clearfield, and M. E. Thompson, *Chem. Mater.* **6,** 1845 (1994).
8. C. Y. Ortiz-Avila and A. Clearfield, *J. Chem. Soc. Dalton Trans.*, 1617 (1989).
9. G. Alberti, S. Murcia-Mascaros, and R. Vivani, *J. Am. Chem. Soc.* **120,** 9291 (1998).
10. G. Alberti, R. Vivani, and S. Murcia-Mascaros, *J. Mol. Struct.* **470,** 81 (1998).
11. G. Alberti, E. Giontella, and S. Murcia-Mascaros, *Inorg. Chem.* **37,** 4672 (1998).
12. G. Alberti, M. Bartocci, M. Santarelli, and R. Vivani, *Inorg. Chem.* **36,** 3574 (1997).
13. G. Alberti, E. Giontella, and S. Murcia-Mascaros, *Inorg. Chem.* **36,** 2844 (1997).
14. G. Alberti, L. Boccali, C. Dionigi, R. Vivani, V. I. Kalchenko, and L. I. Atamas, *Supramol. Chem.* **7,** 129 (1996).
15. G. Alberti, M. Casciola, U. Costantino, and R. Vivani, *Adv. Mater.* **8,** 291 (1996).
16. G. Alberti, F. Marmottini, S. Murcia-Mascaros, and R. Vivani, *Angew. Chem. Int. Ed. Engl.* **33,** 1594 (1994).
17. S. Yamanaka, K. Sakamoto, and M. Hattori, *J. Phys. Chem.* **88,** 2067 (1984).
18. L. A. Vermeulen and M. E. Thompson, *Nature* **358,** 656 (1992).
19. G. Alberti, U. Costantino, and G. J. Perego, *Solid State Chem.* **63,** 455 (1986).
20. G. Alberti and U. Costantino, *J. Mol. Catal.* **27,** 235 (1984).
21. S. G. Bertolotti, J. J. Cosa, H. E Gsponer, and C. M. Previtali, *Can. J. Chem.* **65,** 2425 (1987).
22. A. Nakahara and J. H. Wang, *J. Phys. Chem.* **67,** 496 (1963).
23. L. A. Vermeulen, J. Pattanayak, T. Fisher, M. Hansford and S. J. Burgmeyer, *Mater. Res. Soc. Symp. Proc.* **431,** 271 (1996).
24. A. Dokoutchaev, V. V. Krishnan, M. E. Thompson, and M. Balasubramanian, *J. Mol. Struct.* **470,** 191 (1998).
25. H. Byrd, A. Clearfield, D. Poojary, K. P. Reis, and M. E. Thompson, *Chem. Mater.* **8,** 2239 (1996).
26. H. Byrd, E. P. Suponeva, A. B. Bocarsly, and M. E. Thompson, *Nature* **380,** 610 (1996).
27. M. E. Thompson, J. L. Snover, V. Joshi, and L. A. Vermeulen, U.S. Patent 5,480,629.
28. M. E. Thompson, J. L. Snover, and L. A. Vermeulen, U.S. Patent 5,500,297.